Protection and Delivery of Anthelmintic Protein Cry5B to Nematodes Using Mesoporous Silicon Particles

Chia-Chen Wu,[†] Yan Hu,[‡] Melanie Miller,[‡] Raffi V. Aroian,[‡] and Michael J. Sailor*[,†,§]

[†]Materials Science and Engineering, [‡]Section of Cell and Development Biology, and [§]Department of Chemistry and Biochemistry, University of California, San Diego, La Jolla, California 92093, United States. Present address: R.V.A.: Program in Molecular Medicine, University of Massachusetts Medical School, Worcester, Massachusetts 01605.

ABSTRACT The ability of nano- and microparticles of partially oxidized mesoporous silicon (pSi) to sequester, protect, and deliver the anthelmintic pore-forming protein Cry5B to nematodes is assessed *in vitro* and *in vivo*. Thermally oxidized pSi particles are stable under gastric conditions and show relatively low toxicity to nematodes. Fluorescence images of rhodamine-labeled pSi particles within the nematodes *Caenorhabditis elegans* and *Ancylostoma ceylanicum* show that ingestion is dependent on particle size: particles of a 0.4 ± 0.2 μm size are noticeably ingested by both species within 2 h of introduction *in vitro*, whereas 5 ± 2 μm particles are excluded from *C. elegans* but enter the pharynx region of *A. ceylanicum* after 24 h. The anthelmintic protein Cry5B, a pore-forming crystal (Cry) protein derived from *Bacillus thuringiensis*, is incorporated into the pSi particles by aqueous infiltration. Feeding of Cry5B-loaded pSi particles to *C. elegans* leads to significant intoxication of the nematode. Protein-loaded particles of size 0.4 μm display the highest level of *in vitro* toxicity toward *C. elegans* on a drug-mass basis. The porous nanostructure protects Cry5B from hydrolytic and enzymatic (pepsin) degradation in simulated gastric fluid (pH 1.2) for time periods up to 2 h. *In vivo* experiments with hookworm-infected hamsters show no significant reduction in worm burden with the Cry5B-loaded particles, which is attributed to slow release of the protein from the particles and/or short residence time of the particles in the duodenum of the animal.

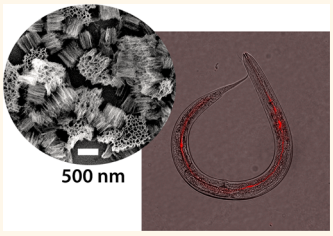

KEYWORDS: porous silicon · oral drug delivery · *C. elegans* · *A. ceylanicum* · hookworm · *Bacillus thuringiensis* (Bt) · crystal protein

Soil-transmitted helminths (STHs) are important parasites of humans, infecting well over 1 billion people worldwide and resulting in marked morbidity, such as malnutrition, anemia, growth stunting, cognitive impairment, school absenteeism, and decreased economic potential for children later in life.[1,2] Current treatment revolves around mass drug administration (MDA) with benzimidazole anthelmintics (primarily albendazole), but widespread anthelmintic resistance in veterinary husbandry and reports of low efficacy of albendazole in human therapy suggest that new anthelmintics are urgently needed.[3,4] One of the more promising new anthelmintics in development for STHs is the crystal (Cry) protein Cry5B, derived from *Bacillus thuringiensis*,[5] which has been shown to be highly effective against *in vivo* infections of STHs such as *Ascaris*[6] and hookworm.[7] Cry5B is a member of the three-domain *B. thuringiensis* Cry proteins, which are pore-forming proteins that target the invertebrate (insect/nematode) intestine, in the case of Cry5B by binding to invertebrate-specific glycolipids present on the apical surface of the nematode intestine.[8]

A substantial challenge in the use of orally delivered protein-based therapeutics for intestinal infections such as Cry5B is the hydrolytic and proteolytic conditions of the stomach, which degrade the therapeutic before it can reach the site of infection. This necessitates administration of a high dose, which introduces additional cost and the increased possibility of toxic side effects. In this work, we evaluate mesoporous silicon microparticles as a nontoxic[9−14] delivery system for the more effective delivery of anthelmintic protein Cry5B.[15] Cry5B toxin is a large (140 kDa) protein composed of three distinct domains, with the overall dimensions of 85 × 65 × 45 Å^3.[16,17] The pore dimensions in electrochemically generated mesoporous Si can be adjusted to a size adequate to admit this protein[13,18,19] but sufficiently small to inhibit the action of

* Address correspondence to msailor@ucsd.edu.

Received for review March 5, 2015 and accepted May 7, 2015.

Published online May 07, 2015
10.1021/acsnano.5b01426

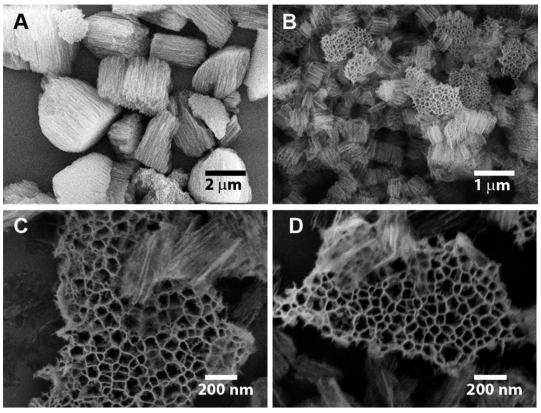

Figure 1. Scanning electron microscope images of the two types of pSi particles used in this study. (A) 5 μm formulation, prior to thermal oxidation. (B) 0.4 μm formulation, prior to thermal oxidation. (C) Closer view of the 0.4 μm formulation revealing the pore morphology, prior to thermal oxidation. (D) Similar view of the 0.4 μm formulation after furnace oxidation at 400 °C for 1 h.

proteolytic enzymes.[20−22] For this study, we investigated a partially oxidized form of pSi because the oxide surface has been shown to be compatible with sensitive proteins,[19,23−31] and the negatively charged surface allows concentration of positively charged proteins in the pores via electrostatic forces.[23,32] Furthermore, oxidized pSi has been shown to be stable under acidic conditions but readily dissolves at pH >7,[33] which is advantageous for an oral route of delivery to the intestines.[29,34]

RESULTS AND DISCUSSION

Morphology of pSi Particles. The pSi particles used in this study were prepared by electrochemical etch of single-crystal silicon wafers. The electrochemical method used to prepare pSi provides good control over particle size and pore size. In this work, two sizes of particles were prepared, of nominal sizes 5 and 0.4 μm (Figure 1A,B). The average pore size in both particle types was approximately ~60 nm (measured from SEM images) for the freshly etched pSi surface (Figure 1C). To improve biocompatibility[35] and protein loading,[23] the particles were oxidized by thermolysis in air at 400 °C. Under these conditions, the pore walls obtain a thin shell of silicon oxide, which is expected to result in an expansion of the pore walls and thus reduction of the average pore diameter. However, because of the relatively wide distribution of pore dimensions in the samples, no obvious decrease in pore dimension was observed in the SEM images of postoxidation samples (Figure 1D). The physical size and the distribution of sizes of the 0.4 μm particles was determined by dynamic light scattering (DLS) and shows a (Z average) particle dimension of 420 nm with a polydispersity index (PdI) of 0.34 for the freshly etched particles. The particle dimensions increased to 580 nm (PdI = 0.46) upon thermal oxidation (Supporting Information Figure S1).

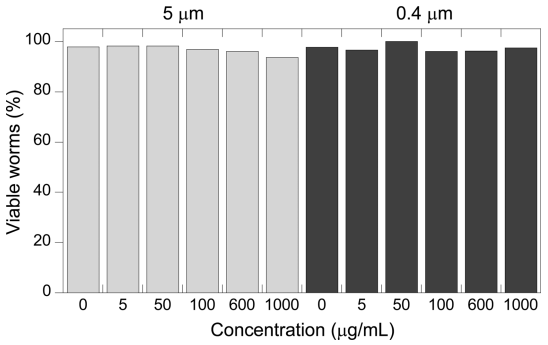

Figure 2. Viability of *C. elegans* incubated with the two different sizes of thermally oxidized pSi particles as a function of particle concentration in the media. Light gray bars correspond to the 5 μm formulation and dark bars correspond to the 0.4 μm formulation used in this work.

The observed increase in average particle size for the oxidized materials is attributed to a small degree of particle aggregation in the DLS experiment. The size distribution of the 5 μm pSi particles was ascertained from statistical analysis of SEM images, yielding an average particle size of 5.8 ± 2.0 μm (Supporting Information Figure S2).

The thermal oxidation procedure removes the surface Si−H species and introduces a surface oxide, as indicated by the infrared spectrum. Vibrational bands associated with surface Si−H species (2109, 2085, 903, and 623 cm^{-1}) are replaced by a strong band associated with Si−O−Si (1058 cm^{-1}) upon oxidation of the particles (Supporting Information Figure S3).

Toxicity of pSi Particles to *Caenorhabditis elegans*. Being sensitive to the majority of anthelmintic drugs that are used against parasitic worm infections of humans and livestock, *Caenorhabditis elegans* serves as a reasonable model for laboratory evaluation of anthelmintic activity.[15] To evaluate their feasibility as delivery vehicles for therapies against parasitic infections, we first characterized the toxicity of the pSi particles (with no drug loaded) to *C. elegans*. The toxicity of mesoporous silicon has been shown to be low in a number of tissue and animal models,[9,11,13,14,36−41] and dissolution of pSi produces orthosilicate ions, the bioavailable form of silicon naturally found in the body.[10] However, its toxicity to nematodes had not previously been assessed.

The toxicity to *C. elegans* of both types of thermally oxidized pSi particles used in this study was assessed with a mortality assay. Particles incubated with *C. elegans* for 6 days at 25 °C showed no major toxicity, as scored by live/dead counts (Figure 2).

Cry5B Protein Loading. Loading of crystal protein anthelmintic Cry5B was achieved by mixing the thermally oxidized pSi particles with Cry5B in a citrate buffer (pH 3.0). At pH 3, the protein is highly soluble and bears a net positive charge (p*I* 5.1), whereas the charge on the oxidized pSi surface is negative.[33] As seen previously with positively charged proteins under similar conditions,[18,22,31,32,42−44] the adsorption of Cry5B onto

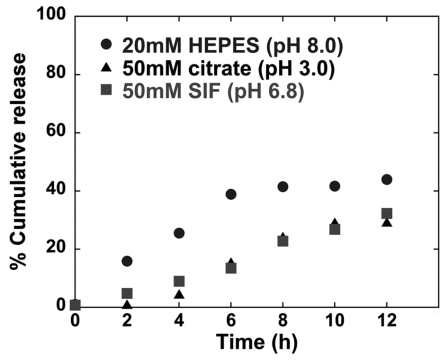

Figure 3. Percent cumulative release of Cry5B from 5 μm pSi particles as a function of time. Release profiles for aqueous 20 mM HEPES buffer (pH 8.0), 50 mM citrate buffer (pH 3.0), and simulated intestinal fluid (SIF) without pancreatin (pH 6.8) are presented as indicated in the legend. All release data were obtained with samples incubated at 37 °C. Concentrations of released Cry5B in each buffer at the indicated time points were quantified using the BCA total protein assay.

the thermally oxidized pSi surface is postulated to occur via electrostatic interaction. The loading efficiency, determined by measuring the difference in protein concentration (BCA assay) in the loading solution before and after loading, was 110 ± 10 μg of Cry5B/mg of pSi, or 10% by mass. Both the 0.4 and 5 μm pSi particle types showed similar loading efficiencies. Loading of Cry5B resulted in a significant increase in the surface charge of the pSi particles: the zeta potential changed from −3.63 to +19.60 mV upon Cry5B loading, which indicates that a significant quantity of protein also coated the exterior surface of the pSi particles.

***In vitro* Release of Cry5B Loaded into pSi Particles.** Temporal release profiles of Cry5B from the 5 μm particle formulation were obtained using three different media that are relevant to *in vitro* assays and the *in vivo* environment (Figure 3). Cry5B is relatively insoluble in water, but it is highly soluble in 20 mM HEPES (pH 8.0) and 50 mM citrate (pH 3.0) buffer solutions. Incubation of the drug-loaded particles in HEPES buffer showed the largest rate of release of Cry5B (44% released in 12 h at 37 °C), whereas the release rates observed in citrate buffer and simulated intestinal fluid were similar to each other and somewhat lower than those in HEPES. These data are consistent with the known dependence of the degradation rate of pSi or oxidized pSi ($pSiO_2$) on pH; silicates and silicon tend to dissolve much more rapidly at pH >7.[34,45]

Potency of Cry5B-Loaded pSi Particles toward *C. elegans*. Activity of Cry5B-loaded pSi particles was assessed by incubation with *C. elegans* and quantified as percent of viable worms after 6 days of incubation at 25 °C. First, in order to identify an optimal particle size, we prepared four different sizes of pSi particles: 0.2, 0.4, 1, and 5 μm. The live/dead ratio for each of these Cry5B-loaded formulations was compared to worms incubated with free Cry5B protein (Figure 4A). The results of control experiments with free Cry5B toward *C. elegans* established an LC_{50} of 2.04 μg/mL, consistent with previous studies. As shown in Figure 4A, four different sizes of Cry5B-loaded pSi particles were tested. The greatest efficacy was seen with the 0.4 μm pSi particle formulation. On a Cry5B mass basis, this formulation was almost as effective as free Cry5B in killing *C. elegans*. It is likely that under these conditions the particles have not released the entire drug payload, but assuming that they have, the 0.4 μm particle−Cry5B formulation appears to retain at least 75% of the activity of the free drug when administered in this assay. The smallest size particles (0.2 μm) showed the least effect, and they appeared to be substantially aggregated relative to the other formulations.

We hypothesize two mechanisms by which the Cry5B-loaded particles kill nematodes: (1) Cry5B first diffuses out of the pSi nanostructure, and then it is ingested by nematodes. (2) Nematodes directly ingest pSi particles containing Cry5B, and the protein is then released inside the midgut of the organism. In control experiments carried out in the culturing medium under the same experimental conditions but in the absence of *C. elegans*, we determined (via BCA assay) that only ∼11% of Cry5B was released from the pSi particles. The relatively low solubility of Cry5B in culture media is probably a contributing factor in limiting the release of Cry5B from the particles and plays a role in the very low level of activity seen for the 0.2 and 5 μm particle formulations. As will be discussed below, the 0.4 and 1 μm particle formulations are sufficiently small to be directly ingested by the nematodes, which provides a second pathway by which Cry5B can reach the midgut of worms. The 0.4 and 1 μm particle formulations did not appear to aggregate, and the 0.4 μm particle formulation showed the greatest efficacy of the four formulations tested. The 0.4 μm particle formulation was therefore selected for further study.

Efficacy of Cry5B-Loaded pSi Particles after Exposure to Gastric Conditions. For oral delivery of therapeutic proteins to parasitic worms residing in the intestine, transit through the gastric fluids of the stomach is a major barrier.[34] Cry5B is susceptible to hydrolytic and enzymatic degradation in simulated gastric fluid (SGF), which would substantially reduce efficacy against worm infestations lower in the gastrointestinal tract. The ability of mesoporous Si to sequester and protect molecules from various degradation pathways has been demonstrated,[23,34] and it appears to be quite effective in the case of the Cry5B protein. We assessed the ability of the pSi host to protect Cry5B in SGF containing pepsin at pH 1.2. The 0.4 μm particle formulation was chosen because it showed the best bioactivity among the four particle sizes tested (Figure 4A). Both free Cry5B and Cry5B-loaded pSi particles were incubated in SGF at 37 °C for 2 h with

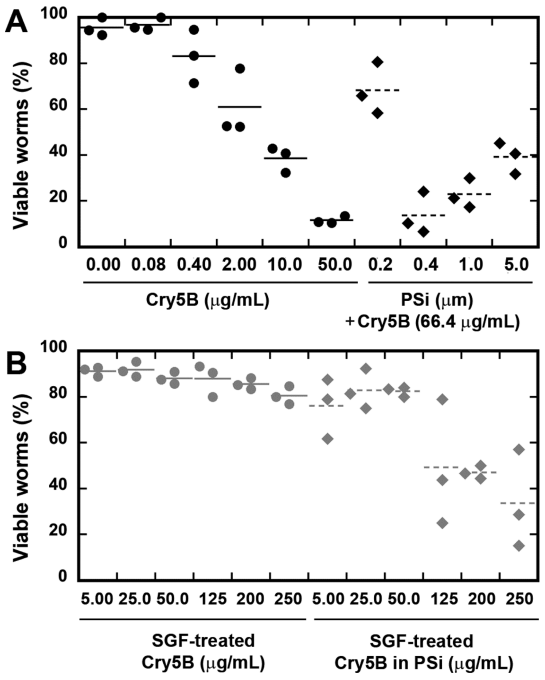

Figure 4. Bioactivity of Cry5B–pSi forumlations toward *C. elegans*, quantified as percent viable worms. (A) Percent viable worms for the 12 conditions of Cry5B tested. First six conditions (solid circles) show dose response of *C. elegans* to purified, unformulated Cry5B protein (no pSi particles) administered at the indicated concentrations. Last four conditions (solid diamonds) consist of Cry5B protein loaded into four different sizes of pSi particles (dimensions 0.2, 0.4, 1, and 5 μm) as indicated. Each particle formulation was administered to the well such that the total concentration of Cry5B protein was 66.4 μg/mL (drug loading efficiency in the particles was 10% by mass, determined in separate experiments). Solid and dashed lines indicate mean % of viable worms from three independent experiments. (Each data point represents an independent experiment averaged for three wells.) 0.4 μm particle formulation shows the greatest efficacy. (B) Percent viable *C. elegans* for 12 different conditions of Cry5B previously exposed to simulated gastric fluid (SGF). Prior to introduction to the worms, each condition was exposed to simulated gastric fluid (pH 1.2) containing pepsin for 2 h. First six conditions (gray circles) show a dose response to the SGF-treated, purified, unformulated Cry5B protein (no pSi particles) administered at the indicated concentrations. Last six conditions (gray diamonds) consist of Cry5B protein loaded into 0.4 μm pSi particles. The amount of Cry5B drug (in μg Cry5B protein per mL of culture medium) for each condition is indicated along the *x* axis. For all experiments, percent viability was assessed after 6 days of incubation with the indicated condition.

mild shaking. After neutralization of acid and pepsin activity, the samples containing either Cry5B or Cry5B-loaded pSi particles were then incubated with *C. elegans*. As expected, free Cry5B protein had no activity against *C. elegans* following SGF treatment even at concentrations up to 250 μg/mL (Figure 4B). By contrast, the Cry5B-loaded 0.4 μm particles displayed significant retention of activity under these conditions, reducing the percent of viable worms to as little as 40% (Figure 4B). These results show that the nanostructure provides substantial protection of the Cry5B payload from the aggressive conditions of SGF. This resistance of the immobilized Cry5B protein to enzymatic attack or hydrolytic degradation is attributed to the limited steric accessibility and shielding afforded by the confines of the ~60 nm pores of the pSi nanostructure.

Size Dependence on pSi Particle Uptake by *C. elegans*. To evaluate the hypothesis that the high efficacy of the 0.4 μm formulation is related to the ability of the nematode to directly ingest the particles, a fluorescent rhodamine-dye tracer was conjugated to the pSi particles and administered to *C. elegans*, which were then investigated by fluorescence microscopy. Rhodamine was chosen to provide spectral separation from the autofluorescence of gut granules in *C. elegans*.[46] The uptake of rhodamine-labeled pSi particles (containing no drug) after 2 h incubation is shown in Figure 5, where the pSi particles (0.4 μm formulation) appear to have lodged in the lumen of the pharynx and the intestine of *C. elegans*. The pSi particles were exclusively found in the primary organs of entry, *e.g.*, the lumen of the digestive tract. No translocation to secondary organs was observed for the 0.4 μm particles. Note the resolution and sensitivity of the microscope used here are such that we cannot comment on the possibility of endocytosis of the particles or completely exclude the possibility of some particle penetration further into *C. elegans*.

The observed location of the pSi particles is consistent with a previous report of the distribution of 50 nm silica-based nanoparticles in *C. elegans*.[47] In that prior study, the nanoparticles were observed to form clumps inside the lumen, similar to the aggregation observed close to the anus in Figure 5D. Similar experiments using the 5 μm pSi formulation showed no detectable uptake under the same exposure (2 h) and imaging conditions, suggesting that these larger particles are not as readily ingested by *C. elegans*. This result is consistent with the reduced ability of the 5 μm pSi formulation to kill *C. elegans* when it is loaded with Cry5B, shown in Figure 4A. Taken together, our data support the hypothesis that direct ingestion of the nanoparticles by the nematodes is an important contributor to the overall efficacy of the Cry5B–pSi construct, with diffusion out of the pSi nanostructure playing a secondary role. However, a more extensive study of the ingestion, aggregation patterns, and dwell time as a function of particle size would be informative.

pSi Particle Uptake by *Ancylostoma ceylanicum*. Because the target of Cry5B therapy is soil-transmitted helminths, of which hookworms are the most important clinically, we studied the interaction of pSi particles *in vitro* on adults of the hookworm *Ancylostoma ceylanicum*. *A. ceylanicum* is a zoonotic hookworm species that is a substantial health problem to humans in Southeast Asia and that is closely related to the major human parasitic nematode *Ancylostoma duodenale*.[48] As with *C. elegans*, ingestion of pSi particles was observed

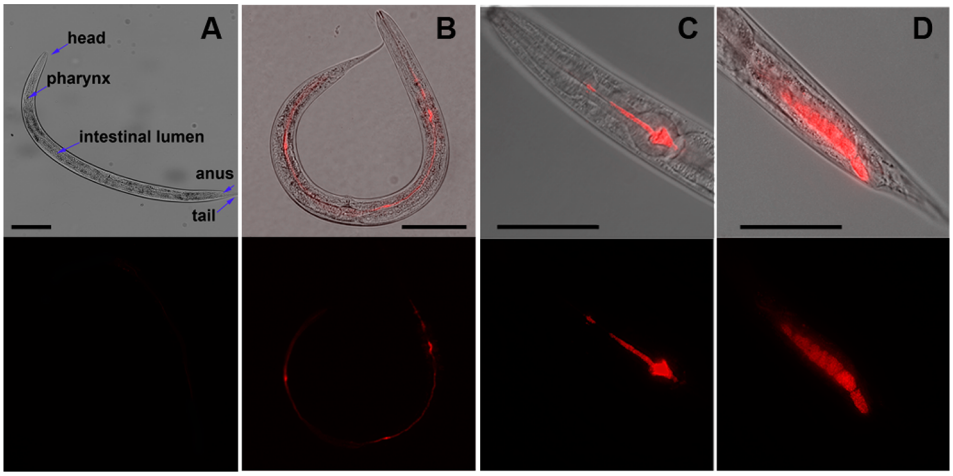

Figure 5. Merged fluorescence/differential interference contrast (top panels) and fluorescence (bottom panels) images of *C. elegans* incubated with rhodamine-labeled pSi nanoparticles. (A) Untreated young adult with the relevant anatomical features indicated. (B) Worm incubated with 0.4 μm rhodamine-labeled pSi particles for 2 h. Rhodamine label can be seen throughout the lumen of the intestine. (C and D) Higher magnification images of pharynx and anus regions of worms treated under the same conditions as in B. Exposure times were identical for images A and B. Scale bars: 50, 50, 100, and 100 μm, for A–D, respectively.

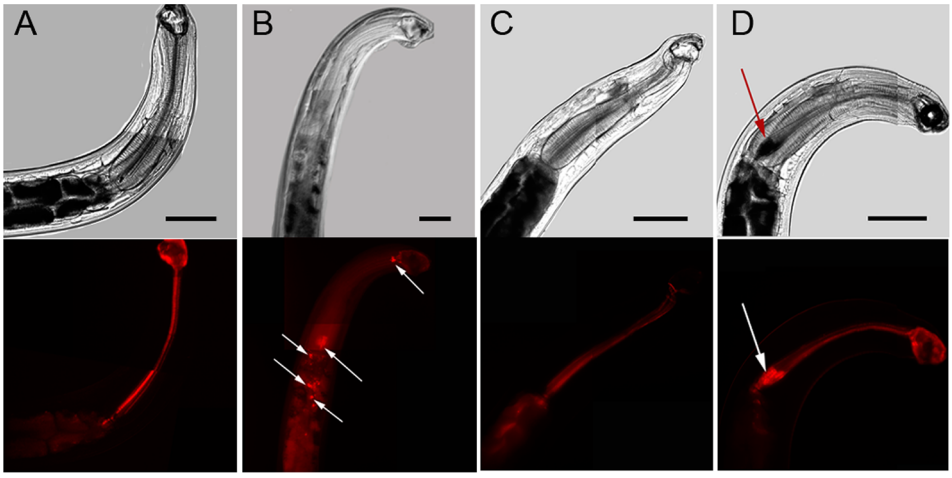

Figure 6. Differential interference contrast (top panels) and fluorescence (bottom panels) images of adult *A. ceylanicum* (hookworm) incubated with rhodamine-labeled pSi particles. (A) Untreated hookworm control. Note strong tissue autofluorescence is observed from the intestine. (B) Worm incubated with 0.4 μm rhodamine-labeled pSi particles for 2 h. White arrows indicate clumps of pSi particles inside the intestinal lumen. (C) Worm incubated with 5 μm rhodamine-labeled pSi particles for 2 h. No obvious signs of labeled particles are observed. (D) Worm incubated with 5 μm rhodamine-labeled pSi particles for 24 h. White arrow indicates clump of pSi particles inside the pharyngeal lumen. Hookworms were treated with deionized water to minimize autofluorescence. Exposure times were identical for each image taken. All scale bars represent 200 μm.

with adult hookworms. Perhaps because of the thicker body of *A. ceylanicum*, strong tissue autofluorescence was observed in the fluorescence microscope images. The pharynx showed the least autofluorescent signal and therefore was chosen for imaging (Figure 6A). The adult hookworms were observed to have ingested the 0.4 μm pSi particle formulation after 2 h incubation (Figure 6B). Similar to the results with *C. elegans*, the larger 5 μm particles were not observed to be ingested after 2 h incubation (Figure 6C). However, after 24 h incubation these larger particles were observed in the pharynx (Figure 6D). As indicated with white arrow in Figure 6D, the large clump of pSi particles was restricted to the pharynx and apparently could not transit into the intestine of hookworm. We also observed retropulsion of pSi clumps inside the pharynx for all hookworms treated under this condition, suggesting the large particles could not pass through the restricted passage to intestine.

Pilot Study of a Single-Dose of Cry5B-Loaded pSi Particles against Hookworm Infection in Hamster. We next tested the impact of Cry5B-loaded particles on worm infections *in vivo*. We chose hookworms because research has shown Cry5B displays a similar mechanism of action on hookworms and *C. elegans*, *e.g.*, the invertebrate-specific glycolipid receptors are functionally similar in

both organisms.[49] We used a 5 μm particle size because preliminary toxicity screens on adult hookworms indicated greater toxicity than the 0.4 μm particles *in vitro* (Supporting Information Figure S4). The pSi particles, loaded with Cry5B (or control unloaded pSi particles), were administered by intragastric gavage to hamsters infected with *A. ceylanicum*, and hamster fecal egg counts and intestinal worm burden were assessed following previously reported protocols.[50] The study included 5−6 hamsters in each group and included naked Cry5B and placebo controls. On day 18 post infection (P.I.), placebo (double-distilled water), 5 μm pSi particles, 5 μm pSi particles loaded with Cry5B, and free Cry5B protein, were dosed *per os* to hookworm-infected hamsters at a dose of 6 mg/kg of Cry5B/hamster body mass. This dose was chosen on the basis of our unpublished data indicating that this level of free Cry5B would give some, but not complete clearance, thus allowing us to potentially detect improved efficacy with any formulation. Fecal egg counts, indicative of adult parasite fecundity in the intestine, were collected right before and for 3 days after treatment (Supporting Information Figure S5). Intestinal worm burdens from each group were also determined on day four post-treatment (Supporting Information Figure S6). As expected, both of these metrics indicated significant reduction in worm burden with the free Cry5B control. However, no statistically significant reduction in worm burden was observed from the Cry5B−pSi particle formulation.

The differences between the *in vitro* results (high anthelmintic efficacy) and the *in vivo* results (no anthelmintic efficacy) can be attributed to a number of factors. A major factor is the difference in time of exposure of the Cry5B−pSi particle formulation to the hookworms. For a relatively low solubility protein payload like Cry5B, the rate of release from a pSi particle is expected to be hindered. As shown in Figure 3, only 44% of the total quantity of Cry5B loaded is released from the pSi formulation in 20 mM HEPES during 12 h incubation at 37 °C, and only 32% is released into simulated intestinal fluid under the same conditions. The release occurs steadily over time.

Although the *in vivo* data represent a negative result, the study points to some very important conclusions about protein−nanoparticle therapeutics against these important intestinal parasites. We attribute the lack of *in vivo* efficacy of the Cry5B−pSi particle formulation with respect to hookworms to the relatively slow dissolution of the pSi particle carrier (Supplemental Figure S7), slow release of Cry5B (Figure 3), slow uptake of particles by the worms (Figure 6), and last, a relatively rapid transit of the particles through the duodenum of the animal. We cannot exclude the possibility that protection from SGF of Cry5B in 5 μm particles used *in vivo* is different than that in 0.4 μm particles tested *in vitro* (Figure 4B), but we do not believe this is a dominant factor. Whereas the *in vitro C. elegans* and hookworm adult assays took place over ≥6 days, enough time for a substantial quantity of Cry5B to be released from the particles, the residence time of the particles *in vivo* was probably too short for the formulation to be effective. In the preliminary *in vitro* assay on *A. celanicum*, pSi particles were allowed to incubate with hookworms up to 7 days before motility scoring, whereas in the *A. ceylanicum*-infected hamsters, pSi particles transited the gastrointestinal tract at the physiologically regulated pace, within 1−2 days. A particular challenge for therapeutics targeting parasitic worms like *A. ceylanicum* is the very short residence time of the therapeutic in the duodenum region of the intestine, where the majority of the worms are located. In humans, the transit time for solids through the duodenum can be as short as a few minutes or even seconds,[51] necessitating either a burst release of payload or a means to slow intestinal transport of the carrier−drug formulation. For example, engineering the surface chemistry of the particles to target mucosal layers (with lectin, for example) may extend retention time in the intestine.[52] Prolonging the residence time in the intestine could also increase the rate of carrier uptake by the parasitic worms; in either case, slowing the transit time of the particle−drug formulation could obviate the need for a specifically triggered burst release of drug. Anyhow, on the basis of our combined *in vitro* and *in vivo* data, we conclude that the porous nanoparticle carrier can protect Cry5B from digestive conditions, but that rapid release or prolonged residence of the particle formulations in the intestine will be critical for Cry5B to display its bioactivity against hookworm infections.

CONCLUSIONS

This study focused on mesoporous silicon (pSi) particles as a protective host for the highly effective but unstable anthelmintic drug crystal protein Cry5B. As an empty drug carrier, the pSi particles themselves showed little to no toxicity to *C. elegans* or *A. ceylanicum*, and they could be loaded with 10% by mass of Cry5B while retaining at least 75% of the drug's activity. The oxide shell on the silicon skeleton of these carriers is apparently highly compatible with Cry5B because it imparted significant stability to the adsorbed protein against hydrolytic (pH 1.2) or enzymatic (pepsin) degradation (conditions that completely deactivate free Cry5B). When loaded with Cry5B, the particles showed substantial toxicity toward nematodes. The toxicity of the drug-loaded formulation against *C. elegans* or *A. ceylanicum* was found to be dependent on particle size and the size of the worm mouth, and ingestion of the entire particle by the worm seems to be an effective pathway for inducing toxicity. For *C. elegans*, a formulation with average particle size of 400 nm was effectively ingested by the L4 stage worm, whereas a 5 μm

formulation was excluded from ingestion. For adult *A. celanicum*, both the 0.4 and 5 μm formulations were observed to be taken up; however, the 5 μm formulation could not reach the intestine and required a substantially longer time to accumulate in the pharynx. Despite the good efficacy shown by the Cry5B-loaded particles *in vitro*, *in vivo* experiments with hookworm-infected hamsters showed no significant reduction in worm burden, which we attribute to the relatively slow release of the drug from the pSi carrier and its relatively rapid transit through the animal, illustrating the importance of matching the time scale of drug release to the residence time of the carrier in the targeted tissues.

METHODS

Chemicals and Materials. ⟨100⟩-oriented, boron-doped p-type silicon wafers of resistivity 0.9−1.0 mΩ cm were obtained from Siltronix, Inc. Absolute ethanol (200 proof) was obtained from Rossville Gold Shield Chemicals. Hydrofluoric acid (48% aqueous, ACS grade) was obtained from Fisher Scientific. Sucrose (crystalline, certified ACS grade) was obtained from Fisher Chemicals. Chemicals 5-(and 6)-carboxytetramethylrhodamine succinimidyl ester (NHS-rhodamine), 1-ethyl-3-(3-(dimethylamino)-propyl)carbodiimide hydrochloride (EDC), and bicinchoninic acid (BCA) protein assay reagent were obtained from Thermo Scientific. Pepsin from porcine gastric mucosa (lyophilized powder, 3200−4500 units/mg protein), sodium azide (≥99.5%), and 3-aminopropyltrimethoxysilane (97%) were obtained from Sigma-Aldrich Chemicals. Sodium hydroxide solution (1.0 M) was obtained from EMD Millipore Chemicals. Recipes for culturing medium, special S medium, M9 medium and hookworm culture medium were obtained from previously described methods.[50,53] Cry5Ba1 protein was purified and prepared as described previously.[54]

Preparation of pSi Particles. pSi particles were prepared by anodic electrochemical etch of highly boron-doped p-type silicon (0.97 mΩ cm resistivity) in a 1:1 v:v solution of 48% aqueous hydrofluoric acid and ethanol. *Caution! HF is highly toxic and contact with skin should be avoided.* A custom-built Teflon etch cell was used, which exposed 8.0 cm^2 of the wafer to the electrolyte.[33] The backside of the wafer was contacted with aluminum foil, and a 28 mm diameter spiral-shaped platinum wire loop was used as the counter electrode. To produce pSi particles with narrow size distributions and high yields, the samples were etched using a perforated etching protocol that introduces high-porosity layers periodically through the porous layer.[55,56] These high-porosity layers act as artificial cleavage planes that are easily fractured by ultrasonication, narrowing the particle size distribution and increasing synthetic yield. For the present work, we used the following protocol: (1) A constant anodic current density of 50 mA/cm^2 was applied for periods of time ranging between 20 or 240 s to generate a pSi layer of thickness between 0.4 and 5.0 μm, respectively. (2) A high current-density pulse (200 mA/cm^2, 0.5 s) was applied to generate a thin, high-porosity "perforation". (3) The current density was then lowered to 50 mA/cm^2 and the process repeated through 5−10 cycles. (4) Finally, the perforated porous film was removed from the substrate by application of a constant current density of 5.0 mA/cm^2 for 60 s in a 1:20 v/v solution of 48% aqueous hydrofluoric acid and ethanol electrolyte, generating a freestanding film approximately 40 μm thick. The low concentration of HF in the "lift-off" solution used in the last step leads to an electropolishing condition, which undercuts the pSi layer allowing easy removal from the Si substrate. The perforated etching and lift-off procedure was repeated ~7 times on a given Si wafer. The resulting pSi layers were rinsed several times with absolute ethanol, placed in absolute ethanol in a vial and fractured into particles by ultrasonication (50T ultrasonic bath, VWR International) for at least 20 h. Particles were then rinsed with ethanol and centrifuged at 5000 rpm for 5 min for collection of 5.0 μm pSi microparticles and 11 000 rpm for 20 min for collection of 0.4 μm pSi nanoparticles.

Characterization of pSi Particles. An FEI XL30 ultrahigh-resolution scanning electron microscope (SEM) operating at an accelerating voltage of 5 kV was used to obtain images of the pSi particles. Samples were not coated with metal or carbon prior to imaging, and low beam currents were used to avoid sample charging artifacts. The surface charge of partially oxidized pSi particles before and after protein loading was measured in 50 mM citrate buffer with a Malvern Instruments Zetasizer ZS90 instrument.

Chemical Modification of pSi Particles. The partially oxidized pSi particles were prepared by thermal oxidation in a muffle furnace (Model FD1545M, Thermo Scientific Inc.) at 400 °C for 1 h in ambient air. Conjugation of rhodamine dye to the thermally oxidized pSi particles was achieved following a previously described method.[57] An aqueous solution (1 M in hydrochloric acid, 1.0 mL) was added to 1.0 mg of partially oxidized pSi particles and shaken for 10 min to activate the surface with hydroxyl species; the particles were then washed with deionized water and ethanol three times each. An aliquot (400 μL) of 1.0% 3-aminopropyltrimethoxysilane in ethanol was added to the particles and shaken for 1 h. The particles were then washed with ethanol three times and suspended in 500 μL of ethanol. Next, aqueous solutions of NHS-rhodamine (10 μL, 2 mg/mL) and EDC (50 μL, 10 mg/mL) were added to the particles, and the mixture was allowed to react for 16 h with constant shaking at room temperature. The rhodamine-labeled pSi particles were then washed with ethanol and deionized water three times.

***C. elegans* Bioactivity Assays.** The *C. elegans* strain Bristol N2 was used in this study. Worms were handled and maintained according to published procedures.[58] Biocompatibility of pSi particles with *C. elegans* was assessed using mortality assays (triplicate wells per trial, two independent trials), and the assays measuring bioactivity of Cry5B-loaded pSi particles (triplicate wells per trial and three independent trials) were carried out as previously described.[59] Briefly, synchronized L4-staged *C. elegans* were pipetted in wells of a 48-well plate with 15−30 nematodes/well in sS medium.[58] Included in each well was *Escherichia coli* as a food source (OP50, 40 μL, OD_{600} = 3.0) and pSi particles as indicated in each experiment. As previously published, lethality assays with purified Cry5B were carried out for 6 days at 25 °C, *i.e.*, the length of time required to achieve near complete killing at higher doses and consistent with dose-dependent lethality experiments involving Cry protein experiments with insects.[60,61] As with the prior published assays, 5-fluoro-2′-deoxyuridine (FUdR) was added to prevent production of progeny over the span of the assay. To maintain moisture in the wells, the plates were wrapped in moist paper towels for the duration of the experiment. At day 6, the mortality of *C. elegans* was scored for dead worms by absence of reaction upon gentle poking.

***In Vitro* and *in Vivo A. ceylanicum* Bioactivity Experiments.** *A. ceylanicum* hookworms were maintained in Syrian hamsters.[49] *In vitro* bioactivity assays on adult *A. ceylanicum* were carried out at 37 °C and scored with a motility index as previously described, where a score of 3 represents vigorous activity and 0 represents immotility even when prodded.[50] All animal experiments were performed under protocols approved by the UCSD Institutional Animal Care and Use Committees (IACUC). All housing and care of laboratory animals used in this study conformed to the NIH Guide for the Care and Use of Laboratory Animals in Research (see document 180F22) and all requirements and regulations issued by the USDA, including regulations implementing the Animal Welfare Act (P.L. 89-544) as amended (see document 18-F23). The bioactivity of

Cry5B-loaded pSi particles was studied on an experimental hookworm infection in hamsters. Cry5B protein concentration was determined by comparing intensity of full-length Cry5B on SDS polyacrylamide gels relative to known quantities of BSA standards. Double-distilled water (ddH_2O), Cry5B, pSi particles, and Cry5B-loaded pSi particles were administered by oral gavage to infected hamsters ($n = 23$). On day 18 post infection (P.I.), infected animals ($n = 6$ in each group, except $n = 5$ for placebo group) were treated *per os* with a total volume of 0.4 mL of the relevant treatment targeting 6 mg Cry5B per kg body weight of hamster. Fecal egg counts were used as an indicator for reproduction capability and worm burden, *i.e.*, remaining living worms inside the hamster intestines, to evaluate the therapeutic effect. Egg counts were carried out as previously described.[50]

Feeding Procedure Used to Track Particle Uptake by Nematodes. Rhodamine-labeled pSi particles were fed to nematode cultures by incubating labeled pSi particles (0.2 mg of particles per mL culture medium) with L4 stage *C. elegans* in M9 buffer containing 100 mM glucose (included in previously published assays[54] to increase *C. elegans* uptake in wells for assays that take place in a short time frame) or with adult *A. ceylanicum* in hookworm culture media.[53] The *C. elegans* mixture was placed on a rocking stage for 2−24 h at room temperature and selected worms were transferred to agarose pads for subsequent fluorescence imaging. A 37 °C, 5% CO_2 incubator was used for *A. ceylanicum* incubation with labeled pSi particles.

Fluorescence Microscopy. Nematodes containing rhodamine-labeled pSi particles were visualized on an Olympus IX70 Delta Vision microscope (Applied Precision, Issaquah, WA, USA) using either Nikon 10× or 40× objective lens and photographed with a CoolSnap HQ^2 CCD camera (PhotoMetrics, Inc., USA). Non-fluorescent images were captured using differential interference contrast (DIC); fluorescent images were deconvolved using the SoftWorx program (Applied Precision). An RD-TR-PE filter (Ex/Em 535/617 nm) was used for fluorescence image acquisition. To prepare specimens for microscopy, 8−10 *C. elegans* or 2 adult *A. ceylanicum* organisms were mounted on 2% agarose pads containing 10 mM sodium azide; a coverslip was overlaid to fix the position of the worms. Images were obtained within 2 h of slide preparation to avoid drying of the agarose pads.

Drug Loading. Thermally oxidized pSi particles (3.0 mg) were suspended in aqueous citrate buffer (300 μL, 50 mM, pH 3.0). An aliquot (1.0 mg/mL) of Cry5B (p*I* ~5.1) in citrate buffer was added to the suspension and placed on a rotator (Model 24, Reliable Scientific, Inc.) for 16 h at room temperature. The particles were collected by centrifugation (10 000 rpm for 10 min). Particles were washed with additional citrate buffer (1 mL) to remove loosely bound Cry5B. The amount of Cry5B loaded into the pSi nanostructure was calculated by subtracting the amount of Cry5B removed in the washing steps from the total amount of Cry5B added to the sample using the bicinchoninic acid (BCA) protein assay. The Cry5B concentrations were determined by measuring the maximum optical absorption at a wavelength of 560 nm on a SpectraMax absorbance spectrometer (Molecular Devices) from a calibration curve assuming Beer's law.

Digestive Fluid for Cry5B Metabolic Fate Study. To evaluate the ability of the pSi matrix to protect Cry5B in the mammalian stomach, Cry5B-loaded pSi particles were incubated in freshly prepared simulated gastric fluid (SGF). The SGF was prepared following the standard recipe of the United States Pharmacopeial Convention: Purified pepsin (3.2 g) derived from porcine stomach mucosa, with an activity of 800 to 2500 units per mg of protein, and NaCl (2.0 g) were dissolved in 7.0 mL of hydrochloric acid and sufficient water to make 1000 mL of solution. The pH was adjusted to 1.2 ± 0.05. Cry5B-loaded pSi particles were added to a solution of SGF (0.5 mL) such that the final concentration of Cry5B was 2.5 mg/mL and incubated at 37 °C with mild agitation. At the 2 h time point, the solution was quenched by neutralization with 0.2 M sodium carbonate.[59] The sample was transported at 0 °C and assayed for viability on *C. elegans* immediately.

***In vitro* Cry5B Release Study.** Cry5B-loaded pSi particles (nominal size = 5 μm) were incubated with 1 mL of medium (equivalent to 0.64 mg/mL silicon concentration) at 37 °C with mild agitation. Three relevant media were chosen for the release study: 20 mM HEPES (pH 8.0), 50 mM citrate buffer (pH 3.0), and simulated intestinal fluid without pancreatin (pH 6.8). The supernatant containing released Cry5B was collected every 2 h and replaced with 1 mL of fresh, temperature-equilibrated media over a 12 h period. Concentrations of the released Cry5B were determined using the BCA protein assay described above. Control BCA assay measurements from (empty) pSi particles incubated in the three separate media were subtracted from the relevant test data to correct for protein concentrations.

Statistical Analysis. All data in this article are expressed as the means ± standard error of the mean. Dose−response curves were plotted using KaleidaGraph v. 4.1.3 (Synergy Software). Significance testing was conducted using a one-tailed *t* test (Microsoft Excel 2011) assuming unequal variances. The LC_{50} values and associated 95% confidence intervals were calculated using the PROBIT algorithm (from the XLSTAT add-on to Microsoft Excel).

Conflict of Interest: The authors declare no competing financial interest.

Acknowledgment. This work was supported by the National Science Foundation under grant DMR-1210417, the National Institute of Allergy and Infectious Diseases, NIH grant 2R01AI056189, and by the Defense Advanced Research Projects Agency (DARPA) under Cooperative Agreement HR0011-13-2-0017. The content of the information within this document does not necessarily reflect the position or the policy of the Government. The authors thank Paterno Castillo and Chris MacIsaac for helpful discussions on the ICP-OES data analysis.

Supporting Information Available: Size distribution of pSi particles of targeted 0.4 and 5.0 μm physical dimensions, infrared spectra of thermally oxidized pSi particles, *in vitro* results of effect of Cry5B-loaded pSi particles on adult *A. ceylanicum*, *in vivo* test results of fecal egg count and worm burden from infected hamsters treated with Cry5B-loaded pSi particles and controls, and temporal dissolution profile of pSi particles. The Supporting Information is available free of charge on the ACS Publications website at DOI: 10.1021/acsnano.5b01426.

REFERENCES AND NOTES

1. Ojha, S. C.; Jaide, C.; Jinawath, N.; Rotjanapan, P.; Baral, P. Geohelminths: Public Health Significance. *J. Infect. Dev. Countries* **2014**, *8*, 005–016.
2. Bleakley, H. Disease and Development: Evidence From Hookworm Eradication in the American South. *Q. J. Econ.* **2007**, *122*, 73–117.
3. Humphries, D.; Simms, B. T.; Davey, D.; Otchere, J.; Quagraine, J.; Terryah, S.; Newton, S.; Berg, E.; Harrison, L. M.; Boakye, D.; Wilson, M.; Cappello, M. Hookworm Infection among School Age Children in Kintampo North Municipality, Ghana: Nutritional Risk Factors and Response to Albendazole Treatment. *Am. J. Trop. Med. Hyg.* **2013**, *89*, 540–548.
4. Geary, T. G. Are New Anthelmintics Needed to Eliminate Human Helminthiases? *Curr. Opin. Infect. Dis.* **2012**, *25*, 709–717.
5. Whalon, M. E.; Wingerd, B. A. Bt: Mode of Action and Use. *Arch. Insect Biochem. Physiol.* **2003**, *54*, 200–211.
6. Urban, J. F. J.; Hu, Y.; Miller, M. M.; Scheib, U.; Yiu, Y. Y.; Aroian, R. V. Bacillus thuringiensis-Derived Cry5B Has Potent Anthelmintic Activity Against Ascaris suum. *PLoS Neglected Trop. Dis.* **2013**, *7*, e2263.
7. Hu, Y.; Aroian, R. V. Bacterial Pore-Forming Proteins as Anthelmintics. *Invertebr. Neurosci.* **2012**, *12*, 37–41.
8. Hu, Y.; Aroian, R. V., Promise of Bacillus thuringiensis Crystal Proteins as Anthelmintics. In *Parasitic Helminths: Targets, Screens, Drugs and Vaccines*; Caffrey, C. R., Ed.; Wiley-VCH Verlag GmbH & Co. KGaA: Weinheim, Germany, 2012; pp 267−281.

9. Canham, L. T. Bioactive Silicon Structure Fabrication Through Nanoetching Techniques. *Adv. Mater.* **1995**, *7*, 1033–1037.
10. Anderson, S. H. C.; Elliott, H.; Wallis, D. J.; Canham, L. T.; Powell, J. J. Dissolution of Different Forms of Partially Porous Silicon Wafers Under Simulated Physiological Conditions. *Phys. Status Solidi A* **2003**, *197*, 331–335.
11. Low, S. P.; Voelcker, N. H.; Canham, L. T.; Williams, K. A. The Biocompatibility of Porous Silicon in Tissues of the Eye. *Biomaterials* **2009**, *30*, 2873–2880.
12. Canham, L. T.; Stewart, M. P.; Buriak, J. M.; Reeves, C. L.; Anderson, M.; Squire, E. K.; Allcock, P.; Snow, P. A. Derivatized Porous Silicon Mirrors: Implantable Optical Components With Slow Resorbability. *Phys. Status Solidi A* **2000**, *182*, 521–5.
13. Anglin, E. J.; Cheng, L.; Freeman, W. R.; Sailor, M. J. Porous silicon in drug delivery devices and materials. *Adv. Drug Delivery Rev.* **2008**, *60*, 1266–1277.
14. Salonen, J.; Kaukonen, A. M.; Hirvonen, J.; Lehto, V. P. Mesoporous Silicon in Drug Delivery Applications. *J. Pharm. Sci.* **2008**, *97*, 632–653.
15. Holden-Dye, L.; Walker, R. J. Anthelmintic Drugs. In *WormBook*; The C. elegans Research Community, Ed.; WormBook, 2007. DOI: 10.1895/wormbook.1.143.1. http://www.wormbook.org.
16. Xia, L.-Q.; Zhao, X.-M.; Ding, X.-Z.; Wang, F.-X.; Sun, Y.-J. The Theoretical 3D Structure of Bacillus thuringiensis Cry5Ba. *J. Mol. Model* **2008**, *14*, 843–848.
17. Hui, F.; Scheib, U.; Hu, Y.; Sommer, R. J.; Aroian, R. V.; Ghosh, P. Structure and Glycolipid Binding Properties of the Nematicidal Protein Cry5B. *Biochemistry* **2012**, *51*, 9911–21.
18. Collins, B. E.; Dancil, K.-P.; Abbi, G.; Sailor, M. J. Determining Protein Size Using an Electrochemically Machined Pore Gradient in Silicon. *Adv. Funct. Mater.* **2002**, *12*, 187–191.
19. Karlsson, L. M.; Schubert, M.; Ashkenov, N.; Arwin, H. Protein Adsorption in Porous Silicon Gradients Monitored by Spatially Resolved Spectroscopic Ellipsometry. *Thin Solid Films* **2004**, *455–456*, 726–730.
20. DeLouise, L. A.; Kou, P. M.; Miller, B. L. Cross-Correlation of Optical Microcavity Biosensor Response With Immobilized Enzyme Activity. Insights Into Biosensor Sensitivity. *Anal. Chem.* **2005**, *77*, 3222–3230.
21. Park, J. S.; Lim, S. H.; Sim, S. J.; Chae, H.; Yoon, H. C.; Yang, S. S.; Kim, B. W. Enhancement of Sensitivity in Interferometric Biosensing by Using a New Biolinker and Prebinding Antibody. *J. Microbiol. Biotechnol.* **2006**, *16*, 1968–1976.
22. Orosco, M. M.; Pacholski, C.; Sailor, M. J. Real-Time Monitoring of Enzyme Activity in a Mesoporous Silicon Double Layer. *Nat. Nanotechnol.* **2009**, *4*, 255–258.
23. Andrew, J. S.; Anglin, E. J.; Wu, E. C.; Chen, M. Y.; Cheng, L.; Freeman, W. R.; Sailor, M. J. Sustained Release of a Monoclonal Antibody from Electrochemically Prepared Mesoporous Silicon Oxide. *Adv. Funct. Mater.* **2010**, *20*, 4168–4174.
24. Chen, M. Y.; Klunk, M. D.; Diep, V. M.; Sailor, M. J. Electric Field Assisted Protein Transport, Capture, and Interferometric Sensing in Carbonized Porous Silicon Films. *Adv. Mater.* **2011**, *23*, 4537–4542.
25. Prestidge, C. A.; Barnes, T. J.; Mierczynska-Vasilev, A.; Skinner, W.; Peddie, F.; Barnett, C. Loading and Release of a Model Protein From Porous Silicon Powders. *Phys. Status Solidi A* **2007**, *204*, 3361–3366.
26. De Stefano, L.; D'Auria, S. Confocal Imaging of Protein Distributions in Porous Silicon Optical Structures. *J. Phys.: Condens. Matter* **2007**, *19*, 395009.
27. Tay, L.; Rowell, N. L.; Lockwood, D. J.; Boukherroub, R. *In Situ* Monitoring of Protein Adsorption on Functionalized Porous Si Surfaces. *J. Vac. Sci. Technol., A* **2006**, *24*, 747–751.
28. DeLouise, L. A.; Miller, B. L. Enzyme Immobilization in Porous Silicon: Quantitative Analysis of the Kinetic Parameters for Glutathione-S-Transferases. *Anal. Chem.* **2005**, *77*, 1950–1956.
29. Foraker, A. B.; Walczak, R. J.; Cohen, M. H.; Boiarski, T. A.; Grove, C. F.; Swaan, P. W. Microfabricated Porous Silicon Particles Enhance Paracellular Delivery of Insulin Across Intestinal Caco-2 Cell Monolayers. *Pharm. Res.* **2003**, *20*, 110–116.
30. Arwin, H.; Gavutis, M.; Gustafsson, J.; Schultzberg, M.; Zangooie, S.; Tengvall, P. Protein Adsorption in Thin Porous Silicon Layers. *Phys. Status Solidi A* **2000**, *182*, 515–20.
31. Zangooie, S.; Bjorklund, R.; Arwin, H. Protein Adsorption in Thermally Oxidized Porous Silicon Layers. *Thin Solid Films* **1998**, *313–314*, 825–830.
32. Chen, M. Y.; Sailor, M. J. Charge-Gated Transport of Proteins in Nanostructured Optical Films of Mesoporous Silica. *Anal. Chem.* **2011**, *83*, 7186–7193.
33. Sailor, M. J. *Porous Silicon in Practice: Preparation, Characterization, and Applications*; Wiley-VCH: Weinheim, Germany, 2012; p 249.
34. Canham, L. T. Nanoscale Semiconducting Silicon as a Nutritional Food Additive. *Nanotechnology* **2007**, *18*, 185704.
35. Wu, E. C.; Andrew, J. S.; Buyanin, A.; Kinsella, J. M.; Sailor, M. J. Suitability of Porous Silicon Microparticles for the Long-Term Delivery of Redox-Active Therapeutics. *Chem. Commun.* **2011**, *47*, 5699–5701.
36. Park, J.-H.; Gu, L.; Maltzahn, G. v.; Ruoslahti, E.; Bhatia, S. N.; Sailor, M. J. Biodegradable Luminescent Porous Silicon Nanoparticles for *in vivo* Applications. *Nat. Mater.* **2009**, *8*, 331–336.
37. Cheng, L.; Anglin, E.; Cunin, F.; Kim, D.; Sailor, M. J.; Falkenstein, I.; Tammewar, A.; Freeman, W. R. Intravitreal Properties of Porous Silicon Photonic Crystals: a Potential Self-Reporting Intraocular Drug Delivery Vehicle. *Br. J. Ophthalmol.* **2008**, *92*, 705–711.
38. Schwartz, M. P.; Derfus, A. M.; Alvarez, S. D.; Bhatia, S. N.; Sailor, M. J. The Smart Petri Dish: A Nanostructured Photonic Crystal for Real-Time Monitoring of Living Cells. *Langmuir* **2006**, *22*, 7084–7090.
39. Mayne, A. H.; Bayliss, S. C.; Barr, P.; Tobin, M.; Buckberry, L. D. Biologically Interfaced Porous Silicon Devices. *Phys. Status Solidi A* **2000**, *182*, 505–13.
40. Bayliss, S. C.; Buckberry, L. D.; Harris, P. J.; Tobin, M. Nature of the Silicon-Animal Cell Interface. *J. Porous Mater.* **2000**, *7*, 191–195.
41. Canham, L. T. Porous silicon as a therapeutic biomaterial. In *Proceedings of 1st Annual International IEEE-EMBS Special Topic Conference on Microtechnologies in Medicine and Biology*, Lyon, France, October 12–14, **2000**; pp 109–112.
42. Schwartz, M. P.; Yu, C.; Alvarez, S. D.; Migliori, B.; Godin, D.; Chao, L.; Sailor, M. J. Using an Oxidized Porous Silicon Interferometer for Determination of Relative Protein Binding Affinity Through Non-Covalent Capture Probe Immobilization. *Phys. Status Solidi A* **2007**, *204*, 1444–1448.
43. Bonanno, L. M.; DeLouise, L. A. Steric Crowding Effects on Target Detection in an Affinity Biosensor. *Langmuir* **2007**, *23*, 5817–5823.
44. Tsargorodskaya, A.; Nabok, A. V.; Ray, A. K. Ellipsometric Study of the Adsorption of Bovine Serum Albumin into Porous Silicon. *Nanotechnology* **2004**, *15*, 703–709.
45. Wu, E. C.; Andrew, J. S.; Cheng, L.; Freeman, W. R.; Pearson, L.; Sailor, M. J. Real-Time Monitoring of Sustained Drug Release Using the Optical Properties of Porous Silicon Photonic Crystal Particles. *Biomaterials* **2011**, *32*, 1957–1966.
46. Clokey, G. V.; Jacobson, L. A. The Autofluorescent "Lipofuscin Granules" in the Intestinal Cells of Caenorhabditis elegans are Secondary Lysosomes. *Mech. Ageing Dev.* **1986**, *35*, 79–94.
47. Pluskota, A.; Horzowski, E.; Bossinger, O.; von Mikecz, A. In Caenorhabditis elegans Nanoparticle-Bio-Interactions Become Transparent: Silica-Nanoparticles Induce Reproductive Senescence. *PLoS One* **2009**, *4*, e6622.
48. Inpankaew, T.; Schär, F.; Dalsgaard, A.; Khieu, V.; Chimnoi, W.; Chhoun, C.; Sok, D.; Marti, H.; Muth, S.; Odermatt, P.; Traub, R. J. High Prevalence of Ancylostoma ceylanicum Hookworm Infections in Humans, Cambodia, 2012. *Emerging Infect. Dis.* **2014**, *20*, 976–82.
49. Hu, Y.; Zhan, B.; Keegan, B.; Yiu, Y. Y.; Miller, M. M.; Jones, K.; Aroian, R. V. Mechanistic and Single-Dose *in vivo* Therapeutic

Studies of Cry5B Anthelmintic Action Against Hookworms. *PLoS Neglected Trop. Dis.* **2012**, *6*, e1900.
50. Hu, Y.; Ellis, B. L.; Yiu, Y. Y.; Miller, M. M.; Urban, J. F.; Shi, L. Z.; Aroian, R. V. An Extensive Comparison of the Effect of Anthelmintic Classes on Diverse Nematodes. *PLoS One* **2013**, *8*, e70702.
51. Weitschies, W.; Kosch, O.; Mönnikes, H.; Trahms, L. Magnetic Marker Monitoring: An Application of Biomagnetic Measurement Instrumentation and Principles for the Determination of the Gastrointestinal Behavior of Magnetically Marked Solid Dosage Forms. *Adv. Drug Delivery Rev.* **2005**, *57*, 1210–1222.
52. Ponchel, G.; Irache, J.-M. Specific and Non-specific Bioadhesive Particulate Systems for Oral Delivery to the Gastrointestinal Tract. *Adv. Drug Delivery Rev.* **1998**, *34*, 191–219.
53. Cappello, M.; Bungiro, R. D.; Harrison, L. M.; Bischof, L. J.; Griffitts, J. S.; Barrows, B. D.; Aroian, R. V. A Purified Bacillus thuringiensis Crystal Protein With Therapeutic Activity Against the Hookworm Parasite Ancylostoma ceylanicum. *Proc. Natl. Acad. Sci. U.S.A.* **2006**, *103*, 15154–15159.
54. Griffitts, J. S.; Whitacre, J. L.; Stevens, D. E.; Aroian, R. V. Bt Toxin Resistance From Loss of a Putative Carbohydrate-Modifying Enzyme. *Science* **2001**, *293*, 860–864.
55. Qin, Z.; Joo, J.; Gu, L.; Sailor, M. J. Size Control of Porous Silicon Nanoparticles by Electrochemical Perforation Etching. *Part. Part. Syst. Charact.* **2014**, *31*, 252–256.
56. Bimbo, L. M.; Sarparanta, M.; Santos, H. A.; Airaksinen, A. J.; Mäkilä, E.; Laaksonen, T.; Peltonen, L.; Lehto, V.-P.; Hirvonen, J.; Salonen, J. Biocompatibility of Thermally Hydrocarbonized Porous Silicon Nanoparticles and their Biodistribution in Rats. *ACS Nano* **2010**, *4*, 3023–3032.
57. Meade, S. O.; Chen, M. Y.; Sailor, M. J.; Miskelly, G. M. Multiplexed DNA Detection Using Spectrally Encoded Porous SiO_2 Photonic Crystal Particles. *Anal. Chem.* **2009**, *81*, 2618–2625.
58. Hu, Y.; Xiao, S.-H.; Aroian, R. V. The New Anthelmintic Tribendimidine is an L-type (Levamisole and Pyrantel) Nicotinic Acetylcholine Receptor Agonist. *PLoS Neglected Trop. Dis.* **2009**, *3*, e499.
59. Hu, Y.; Georghiou, S. B.; Kelleher, A. J.; Aroian, R. V. Bacillus thuringiensis Cry5B protein is highly efficacious as a single-dose therapy aginst an intestinal roundworm infection in mice. *PLoS Neglected Trop. Dis.* **2010**, *4*, e614.
60. Bischof, L. J.; Huffman, D. L.; Aroian, R. V., Assays for Toxicity Studies in C. elegans With Bt Crystal Proteins. In *C. elegans: Methods and Applications*, Strange, K., Ed.; Springer: Switzerland, 2006; Vol. 351, pp 139–154.
61. Kao, C. Y.; Los, F. C. O.; Huffman, D. L.; Wachi, S.; Kloft, N.; Husmann, M.; Karabrahimi, V.; Schwartz, J. L.; Bellier, A.; Ha, C.; Sagong, Y.; Fan, H.; Ghosh, P.; Hsieh, M.; Hsu, C. S.; Chen, L.; Aroian, R. V. Global Functional Analyses of Cellular Responses to Pore-Forming Toxins. *PLoS Pathog.* **2011**, *7*, 17.